Supporting Information

Appendix S1: Excluding adults and calculating relative species-level $R_{0,s,p}$

Our sampling protocol did not systematically sample adult amphibians, even if they were present at a site. If adult amphibians were important, but unobserved contributors to Bd dynamics within a season, then our estimates of absolute, species-level $R_{0,s,p}$ values could be biased. Analysis of adults that were haphazardly sampled during surveys suggested that adults tended to have higher mean Bd loads than larvae and that differences in prevalence between adults and larvae varied by species. Given that the density of larval amphibians is typically higher than adults after breeding given the large number of eggs produced by gravid females (from tens to thousands of eggs, Stebbins & McGinnis 2012), it is hard to precisely say whether adults are significant contributors to within-season Bd dynamics and we expect that the contribution of adults could vary by patch and species. Because of this ambiguity, we performed both a relative and absolute analysis of species-level $R_{0,s,p}$, recognizing that the unknown contribution of adults on within-season Bd dynamics could potentially limit our inference on absolute $R_{0,s,p}$ values. Similarly, our study design focused on sampling late-stage larvae and metamorphosing amphibians, but did not sample early-stage larvae. This could also limit our inference on absolute $R_{0,s,p}$ values if early-stage larvae show significantly different infection patterns than late-stage larvae. While we suspect this is unlikely for the five native amphibian species that metamorphose within the same season, the long tadpole stage of *R. catesbeiana* could lead to differences in infection patterns between early- and late-stage tadpoles. However, as we describe below, our inference on *relative* $R_{0,s,p}$ values are robust to the exclusion of particular life stages or species.

Calculating relative $R_{0,s,p}$

Consider the following equation for $R_{0,s,p}$ based on equation 1 in the main text

$$R_{0,s,p} = \frac{\beta_{sp}\lambda_s N^*_{sp}}{b_{sp}\gamma_p} = \frac{1 + \frac{\phi_s}{b_{sp}} \sum_{j \in \text{Patches}} (c_{jp} - c_{pj} \frac{A_j}{A_p} \frac{\Pi^*_{sj}}{\Pi^*_{sp}} \frac{N^*_{sj}}{N^*_{sp}})}{(1 - \Pi^*_{sp})(\sum_{i \in \text{Species}} \frac{\lambda_{ip}}{\lambda_{sp}} \frac{\Pi^*_{ip}}{\Pi^*_{sp}} \frac{N^*_{ip}}{N^*_{sp}})} \tag{S1}$$

A useful property of this equation is that ratios of $R_{0,s,p}$ between two species within a patch only depend on the two species being compared. To illustrate this, consider two species, 1 and 2, in patch p. Let $W_{sp} = \frac{\phi_s}{b_{sp}} \sum_{j \in \text{Patches}} (c_{jp} - c_{pj} \frac{A_j}{A_p} \frac{\Pi^*_{sj}}{\Pi^*_{sp}} \frac{N^*_{sj}}{N^*_{sp}})$ and $F_{sp} = \lambda_{sp} \Pi^*_{sp} N^*_{sp}$. We can write $\frac{R_{0,1,p}}{R_{0,2,p}}$ as

$$\frac{R_{0,1,p}}{R_{0,2,p}} = \left(\frac{1+W_{1p}}{1+W_{2p}}\right)\left(\frac{1-\Pi^*_{2p}}{1-\Pi^*_{1p}}\right)\left(\frac{\frac{1}{F_{2p}}\sum_{i\in\text{Species}} F_{ip}}{\frac{1}{F_{1p}}\sum_{i\in\text{Species}} F_{ip}}\right) \tag{S2}$$

which simplifies to

$$\frac{R_{0,1,p}}{R_{0,2,p}} = \left(\frac{1+W_{1p}}{1+W_{2p}}\right)\left(\frac{1-\Pi^*_{2p}}{1-\Pi^*_{1p}}\right)\left(\frac{F_{1p}}{F_{2p}}\right) \tag{S3}$$

Equation S3 shows that the ratio of species-level $R_{0,s,p}$ only depends on the parameters of the two species being compared. This result is useful because if species or life stages other than 1 and 2, for example, were not sampled in a community, their omission would not affect the calculation of relative $R_{0,s,p}$ ratios.

Appendix S2: The endemic equilibrium assumption

In this study, infection was sampled only once per year for a given pond and thus could not conclusively test whether or not particular patches were in approximate equilibrium within a season. However, Fenton *et al.* (2015) showed that calculations of R_0 using this approach are relatively robust to deviations from the equilibrium assumption if prevalence and host density are fluctuating about a mean value through time. Biologically, our sampling period was generally after the influx of adult amphibians for breeding and before the efflux of metamorphs from the pond, such that we did not expect densities to vary drastically within the sampling period. Moreover, pooling prevalence estimates across the sampled months showed no consistent peaks in prevalence during the sampling season for the six species considered (Fig. S2), suggesting that an approximate endemic equilibrium assumption is not strongly violated for this system.

Appendix S3: Estimating parameters from data

Prevalence and Bd load

We used the Bd survey data described in the main text to estimate two sets of parameters: prevalences Π_{sp} and shedding rate ratios $\frac{\lambda_{ip}}{\lambda_{sp}}$. Based on previous work in other amphibian Bd systems, we assumed that host shedding rate was proportional to Bd load (DiRenzo *et al.* 2014) and estimated the shedding rate ratios for species s and i in patch p as the ratio between estimated mean Bd loads for species s and i in patch p.

We used the methods developed in previous studies to account for false absences and measurement error when estimating species-level mean prevalence and Bd load from the survey data (Miller *et al.* 2012; DiRenzo *et al.* 2018). We accounted for false absences by modeling true prevalence in species s and patch p ($\zeta_{s,p}$) as

$$\sum_{j=1}^{t_i} \mathbb{1}_{y_{ij}>0} \sim \text{Binomial}(z_i p_i^*, t_i) \tag{S4}$$

$$\text{logit}(p_i^*) = \eta_1 + \eta_2 \log(x_i) \tag{S5}$$

$$z_i \sim \text{Bernoulli}(\zeta_{sp}) \tag{S6}$$

where z_i was the true infection state of host i, $\mathbb{1}_{y_{ij}>0}$ was a indicator variable that was one if the Bd load for host i on swab j was greater than zero and zero otherwise, t_i was the number of swabs for host i (three swabs per host in our data), η_2 determined how logit detection probability p_i^* changed with true load x_i, and η_1 was the intercept. Because detection probability p_i^* describes the probability of correctly detecting Bd presence on a host, $1 - p_i^*$ describes the probability of a false absence for host i.

We modeled true prevalence $\zeta_{s,p}$ as

$$\begin{aligned} \text{logit}(\zeta_{s,p}) &= \kappa_0 + \omega_{\text{species}[s]} + \omega_{\text{patch}[p]} + \omega_{\text{patch}\times\text{species}[sp]} \\ \omega_{\text{species}[s]} &\sim N(0,3) \\ \omega_{\text{patch}[p]} &\sim N(0,3) \\ \omega_{\text{patch}\times\text{species}[sp]} &\sim N(0,3) \end{aligned} \tag{S7}$$

where $\omega\cdot$ were normally distributed random effects. We were unable to infer both the variance in the prevalence random effects $\omega\cdot$ and the variance in the Bd load random effects $\alpha\cdot$ (see below). Therefore, we fixed the variance of the prevalence random effects $\omega\cdot$ at a standard deviation of three to allow particular random effects of prevalence to potentially take a large range of values. The parameter κ_0 was the baseline logit prevalence.

We modeled the true Bd load x_i on host i as

$$\log(x_i) \sim \text{Normal}(\tau_{sp}, \sigma_{\text{process}}) \tag{S8}$$

where the true mean log load τ_{sp} was a function of species s in patch p and σ_{process} was the standard deviation of true Bd load. Specifically,

$$
\begin{aligned}
\tau_{sp} &= \tau_0 + \alpha_{\text{species}[s]} + \alpha_{\text{patch}[p]} + \alpha_{\text{patch}\times\text{species}[sp]} \\
\alpha_{\text{species}[s]} &\sim N(0, \sigma_{\text{species}}) \\
\alpha_{\text{patch}[p]} &\sim N(0, \sigma_{\text{patch}}) \\
\alpha_{\text{patch}\times\text{species}[sp]} &\sim N(0, \sigma_{\text{species}\times\text{patch}}) \\
\sigma_{\text{species}}, \sigma_{\text{patch}}, \sigma_{\text{species}\times\text{ patch}} &\sim \text{Half-Normal}(0, 3)
\end{aligned}
\tag{S9}
$$

where $\alpha_{\cdot}$ were normally distributed random effects with different variances. The parameter τ_0 was baseline log Bd load. The parameters $\sigma_{\cdot}$ were standard deviations of the random effects.

Finally, we accounted for qPCR measurement error of Bd load by modeling the observed load y_{ij} on swab j of host i as

$$
\begin{aligned}
\log(y_{ij}) &\sim \text{Normal}(\log(x_i), \sigma_{\text{measurement}}) \text{ if } y_{ij} > 0 \\
\sigma_{\text{measurement}} &\sim \text{Half-Normal}(0, 1)
\end{aligned}
\tag{S10}
$$

The parameter $\sigma_{\text{measurement}}$ was the standard deviation of the measurement error.

We fit the model using a Bayesian framework in the probabilistic programming language Stan. We fit four chains of 1000 samples with a warm-up of 500 samples using Hamiltonian Monte Carlo. We fit Bd survey data from each year separately. We used the estimated true loads $\exp(\tau_{sp})$ and prevalences ζ_{sp} directly with equation 2 in the main text to calculate relative and absolute species-level $R_{0,s,p}$. The Stan code for fitting the model is provided at `https://doi.org/10.25349/D9W59R`.

Estimating host density from amphibian surveys

We modeled the density of amphibian species s at pond p (N^*_{sp}) using a multi-level model described in Joseph *et al.* (2016). We followed the notation of Joseph *et al.* (2016) for consistency and thus re-used some of the symbols defined in the previous section and elsewhere in manuscript. We re-define these symbols in this section as they are re-used. Let y^*_{psj} be the sampled host abundance from sweep j of host s in pond p. The model for host density is given by

$$
y^*_{psj} \sim \begin{cases} \psi_{ps}\text{Poisson}(y^*_{psj}|\theta_{psj}) & \sum_{j=1}^{J_p} y^*_{psj} > 0 \\ \psi_{ps}\text{Poisson}(0|\theta_{psj}) + 1 - \psi_{ps} & \text{otherwise} \end{cases}
\tag{S11}
$$

where J_p is the total number of sweeps in patch p and ψ_{ps} is the probability of true occupancy of host species s at site p. The model assumes that the probability of occupancy increases with host density following $\log(\psi_{ps}) = \gamma_{0s} + \gamma_1 \log(\theta_{ps})$. The parameter γ_{0s} is a host-specific intercept and γ_1 determines the

relationship between log host density and occupancy probability.

The mean abundance θ_{psj} of host s in patch p in sweep j depends on host-, site-, and sweep-specific factors, where α_{0s}, α_{ps}, and α_{js} are random effects on host density for host s, in patch p, on sweep j. Given a mean community abundance of β_c, we can write the log mean abundance as

$$\log(\theta_{psj}) = \beta_c + \alpha_{0s} + \alpha_{ps} + \alpha_{js} \tag{S12}$$

where $\alpha_{0s} \sim N(0, \sigma_{\text{host}})$, $\boldsymbol{\alpha}_p \sim N_H(\mathbf{0}, \Sigma_{\text{patch}})$, and $\boldsymbol{\alpha}_j \sim N_H(\mathbf{0}, \Sigma_{\text{sweep}})$, where $N_d(\mathbf{0}, \Sigma)$ is a multivariate normal distribution of dimension d with a mean vector of zero and a covariance matrix Σ. The random effect $\boldsymbol{\alpha}_p$ is a vector of dimension H species sampled from a multivariate normal distribution and indicates that the densities of host species may covary among patches according to Σ_{patch}. Similarly, the random effect $\boldsymbol{\alpha}_j$ is vector of dimension H species sampled from a multivariate normal distribution and indicates that host densities may covary among sweeps according to Σ_{sweep} (Joseph *et al.* 2016).

When fitting the model, we decomposed the covariance matrix Σ_* into $\text{diag}(\boldsymbol{\sigma})\boldsymbol{\Omega}\text{diag}(\boldsymbol{\sigma})'$ where $\text{diag}(\boldsymbol{\sigma})$ was a diagonal matrix of standard deviations and $\boldsymbol{\Omega}$ was the correlation matrix. The prior distributions on the parameters were (Joseph *et al.* 2016)

$$\begin{aligned}
\beta_c &\sim N(0,1) \\
\sigma_{\text{host}} &\sim \text{Half-Normal}(0,1) \\
\boldsymbol{\Omega}_{\text{patch}}, \boldsymbol{\Omega}_{\text{sweep}} &\sim LKJ(2) \\
\log(\sigma_{ps}) &\sim N(\mu_{\text{patch}}, \sigma_\tau) \\
\log(\sigma_{js}) &\sim N(\mu_{\text{sweep}}, \sigma_\tau) \\
\mu_{\text{patch}} &\sim N(0,1) \\
\mu_{\text{sweep}} &\sim N(0,1) \\
\sigma_\tau &\sim \text{Half-Normal}(0,1) \\
\gamma_{0s} &\sim N(\mu_{\text{occupancy}}, \sigma_{\text{occupancy}}) \\
\mu_{\text{occupancy}} &\sim N(0,1) \\
\sigma_{\text{occupancy}} &\sim \text{Half-Normal}(0,1) \\
\gamma_1 &\sim N(1,1)
\end{aligned} \tag{S13}$$

The prior $\log(\sigma_{ps}) \sim N(\mu_{\text{patch}}, \sigma_\tau)$ is describing the distribution of species-specific standard deviations in patch p. These log standard deviations are drawn from a normal distribution with mean μ_{patch} and a standard

deviation of σ_τ. The prior distribution $\log(\sigma_{js}) \sim N(\mu_{\text{sweep}}, \sigma_\tau)$ is similar, but is describing species-specific standard deviations within a sweep j. The other $\sigma_\cdot$ parameters all describe standard deviations of different random effects in the model.

We fit the model using a Bayesian framework in the probabilistic programming language Stan. We fit four chains of 1000 samples with a warm-up of 500 samples using Hamiltonian Monte Carlo. We fit host density data from each year separately (2013-2018). Stan code for fitting the model is provided by Joseph *et al.* (2016).

Appendix S4: Including connectivity into multi-species, multi-patch metacommunity models

Given a set of connected patches, there were multiple connectivity parameter sets that were equally "plausible" given observed patterns of prevalence, Bd loads, and host density. By "plausible" we mean that $R_{0,s,p} \geq 0$ for all species and patches in the metapopulation. For example, assuming no dispersal always provides a plausible solution to equation S1. To address this challenge, we explored the plausible set of connectivity parameters to determine how the maintenance potential of a species and source potential of a patch varied over the plausible parameter space. Here, we described how we parameterized the connectivity portion of the multi-species, multi-patch model.

We defined species-specific connectivity parameters $c_{s,jp}$. The parameter $c_{s,jp}$ defined the probability of a host species s moving from patch p to patch j conditional on dispersal. We defined the probability of moving from patch p to patch j as normalized exponential decay functions based on the Haversine distance D_{jp} between patch p and j $\frac{a_s \exp(-a_s D_{jp})}{\sum_{m \in P, m \neq p} a_s \exp(-a_s D_{mp})}$ (Hanksi 1999). We normalized the probabilities to one to ensure that an amphibian moved somewhere when it moved. We set the species-specific distance-decay parameter a_s to (0.5 × the maximum dispersal distance observed for a species in the literature)$^{-1}$ to capture the relative propensity of different amphibian species to disperse different distances. The maximum dispersal distances we used were *P. regilla* = 2 km (Smith & Green 2005), *A. boreas* = 6 km (Smith & Green 2005), *R. catesbeiana* = 1.6 km (Smith & Green 2005), *R. draytonii* = 2.8 km (Fellers & Kleeman 2007), *T. torosa* = 4 km (Marsh & Trenham 2001), and *T. granulosa* = 1.6 km (Pimentel 1960).

An important unknown connectivity parameter in the model was the ratio between species-specific dispersal rate and the loss rate from the infected class, $r_{sp} = \phi_s / b_{sp}$. This parameter gives the expected number of patches to which an infected individual of species s that disperses from patch p moves to over its time infected. As this parameter could not be uniquely inferred from snapshot data, we instead allowed r_{sp} to

vary across all species and patches within a metapopulation and explored how species maintenance potential and patch source potential changed across plausible values of r_{sp}, compared to an assumption of no dispersal (i.e. $r_{sp} = 0$).

While the minimum plausible value for r_{sp} was zero for all species and patches, the maximum value for r_{sp} varied by species and patch. We calculated the maximum r_{sp} value for species s in patch p by setting equation S1 to zero and solving for $r_{sp} = \frac{\phi_s}{b_{sp}}$. Doing this, we obtained

$$r_{sp,\max} = \left(\sum_{j \in \text{Patches}} c_{pj} \frac{A_j}{A_p} \frac{\Pi^*_{sj}}{\Pi^*_{sp}} \frac{N^*_{sj}}{N^*_{sp}} - 1 \right)^{-1} \tag{S14}$$

When $\sum_{j \in \text{Patches}} c_{pj} \frac{A_j}{A_p} \frac{\Pi^*_{sj}}{\Pi^*_{sp}} \frac{N^*_{sj}}{N^*_{sp}} > 1$, $r_{sp} > 0$ and there is a maximum plausible r_{sp}, above which $R_{0,s,p} < 0$. When $\sum_{j \in \text{Patches}} c_{pj} \frac{A_j}{A_p} \frac{\Pi^*_{sj}}{\Pi^*_{sp}} \frac{N^*_{sj}}{N^*_{sp}} \leq 1$ there is no maximum r_{sp}, such that r_{sp} can take any value between $(0, \infty)$ and $R_{0,s,p} > 0$.

Biologically, equation S14 tells us something useful about how we would expect plausible $r_{sp,\max}$ values to vary with properties of a population within patch. Consider, without loss of generality, a single species in a metapopulation with equally sized and equally connected patches (i.e. $\frac{A_j}{A_p} = 1$ for all j and $c_{pj} = c_{pi}$ for all $i, j \neq p$). If we observed a patch with low prevalence and low host density relative to other patches in the metapopulation at equilibrium (let's call it 'weak patch'), then the only way the observed prevalence and density patterns could be possible would be if 1.) species dispersal (ϕ_s) was low or 2.) hosts lost infection or died at a high rate within 'weak patch' (b_{sp} was high). Either of these scenarios would lead to a low maximum plausible r_{sp} in 'weak patch'. In contrast, consider a patch with high prevalence and high host density relative to other patches in the metapopulation (let's call it 'strong patch'). If 'strong patch' had sufficiently higher density and prevalence than other patches on the landscape (specifically, such that $\sum_{j \in \text{Patches}} c_{pj} \frac{A_j}{A_p} \frac{\Pi^*_{sj}}{\Pi^*_{sp}} \frac{N^*_{sj}}{N^*_{sp}} \leq 1$), then 'strong patch' would be driving the pathogen dynamics on the landscape. In other words, 'strong patch's contributions to density and prevalence in other patches would be much more than other patches contributions to density and prevalence within 'strong patch'. Therefore, it does not matter how large r_{sp} is for 'strong patch', because there is no expectation that observed prevalence or density in 'strong patch' needs to conform to other patches on the landscape when patches are tightly connected (i.e. r_{sp} is high).

We applied equation S14 to all species in all patches in all metacommunities (1135 species by patch by metacommunity combinations, e.g. *A. boreas* in patch 1 in metacommunity 2) and found that 37% of species by patch by metacommunity combinations were 'strong patches' with no empirical constraint on r_{sp} (i.e. $r_{sp} \in (0, \infty)$ for 37% of the patches). The other 63% of species by patch combinations were 'weak patches'

where maximum r_{sp} was constrained. For 89% of the 'weak patches', constrained maximum r_{sp} values were predicted to be less than one. This amounted to 56% of the 1135 species by patch by metacommunity r_{sp} values being restricted to less than one.

Using this information, for each metacommunity with H species and P patches we drew $H \times P$ r_{sp} parameters uniformly between zero and $\min(r_{sp,\max}, 1)$ and computed the species-level $R_{0,s,p}$ for all species and patches in a metacommunity using equation S1. We assumed that plausible values of r_{sp} would not be greater than one for three reasons. First, the above analysis showed that over half of $r_{sp,\max}$ values were constrained to be less than one strictly based on the observed data. Second, larvae and metamorphs were the most abundant life stages present in a pond during sampling and these life stages disperse little if at all before maturing into juveniles and adults. Therefore, we would expect within-season dispersal rate to be low. Third, 90% of the observed Bd loads were less than 500 zoospores and previous studies have shown that even susceptible species can clear infections when loads are less than or equal to 500 zoospores (e.g. Wilber *et al.* 2016; Ohmer *et al.* 2017). This suggests that Bd loss rates are likely high relative to dispersal rates such that r_{sp} is less than one. As a sensitivity analysis, we also explored allowing r_{sp} to vary uniformly between 0 and $\min(r_{sp,\max}, 10)$ and our general results were unchanged.

Appendix S5: Computing landscape-level $R_{0,L}$

The landscape-level $R_{0,L}$ for equation 1 in the main text defines the average number of infected hosts produced by an average infected host in a fully susceptible metacommunity. Using the next-generation matrix approach (Diekmann *et al.* 1990), $R_{0,L}$ can be calculated as

$$R_{0,L} = \max \text{ eig}(\mathbf{R}(-\mathbf{B})^{-1}) \tag{S15}$$

where

$$\mathbf{R} = \begin{bmatrix} R_1 & 0 & \cdots & 0 \\ 0 & R_2 & \cdots & 0 \\ \vdots & \vdots & \vdots & \vdots \\ 0 & 0 & \cdots & R_P \end{bmatrix} \tag{S16}$$

The variable P gives the number of patches in a metacommunity and H gives the total number of host species. The sub-matrix R_j is given by

$$R_j = \begin{bmatrix} R_{0,1,j}\frac{\lambda_{1j}}{\lambda_{1j}}b_{1j} & R_{0,1,j}\frac{\lambda_{2j}}{\lambda_{1j}}b_{1j} & \cdots & R_{0,1,j}\frac{\lambda_{Hj}}{\lambda_{1j}}b_{1j} \\ \vdots & \vdots & \vdots & \vdots \\ R_{0,H,j}\frac{\lambda_{1j}}{\lambda_{Hj}}b_{Hj} & R_{0,H,j}\frac{\lambda_{2j}}{\lambda_{Hj}}b_{Hj} & \cdots & R_{0,H,j}\frac{\lambda_{Hj}}{\lambda_{Hj}}b_{Hj} \end{bmatrix} \tag{S17}$$

177 $R_{0,i,j}$ is the species-level R_0 for species i in patch j.

178 The matrix $\mathbf{B}$ defines how infected hosts in the metacommunity transition while in the infected class.
179 This could mean leaving the infected class or moving to another patch. $\mathbf{B}$ can be defined by the square
180 sub-matrices

$$\mathbf{B} = \begin{bmatrix} D_1 & E_{12} & \ldots & E_{1P} \\ E_{21} & D_2 & \ldots & E_{2P} \\ \vdots & \vdots & \vdots & \vdots \\ E_{P1} & E_{P2} & \ldots & D_P \end{bmatrix} \tag{S18}$$

181 D_p for patch p is a diagonal $H \times H$ matrix

$$D_p = \begin{bmatrix} -b_{1p} - \phi_1 \sum_{i=1}^{P} c_{i,p} & 0 & \ldots & 0 \\ 0 & -b_{2p} - \phi_2 \sum_{i=1}^{P} c_{i,p} & \ldots & 0 \\ \vdots & \vdots & \vdots & \vdots \\ 0 & 0 & \ldots & -b_{Hp} - \phi_H \sum_{i=1}^{P} c_{i,p} \end{bmatrix} \tag{S19}$$

182 where $\sum_{i=1}^{P} c_{i,p} = 1$ given that $c_{i,p}$ defines the probability of moving from patch p to i, conditional on a
183 host moving somewhere (see equation 1 in the main text). b_{1p} is the rate that infected individuals of species
184 1 in patch j leave the infected class. This could be due to recovery, natural mortality, or disease-induced
185 mortality.

186 E_{ip} is the diagonal $H \times H$ matrix

$$E_{ip} = \begin{bmatrix} \frac{A_p}{A_i}c_{ip}\phi_1 & 0 & \ldots & 0 \\ 0 & \frac{A_p}{A_i}c_{ip}\phi_2 & \ldots & 0 \\ \vdots & \vdots & \vdots & \vdots \\ 0 & 0 & \ldots & \frac{A_p}{A_i}c_{ip}\phi_H \end{bmatrix} \tag{S20}$$

187 where $\frac{A_p}{A_i}$ is the ratio of patch areas for patch p and i and ϕ_s is the dispersal rate of species s. Note that
188 parameters c_{ip} could be made species-specific by writing $c_{s,ip}$.

189 Inspection of the matrix $\mathbf{K} = \mathbf{R}(-\mathbf{B})^{-1}$, shows that all entries in K can be re-written in terms of ratios

$\phi_s/b_{sp} = r_{sp}$ and b_{sp}/b_{tq} for $s, t = 1, \ldots, H$ and $p, q = 1, \ldots, P$. Therefore, the only additional information needed to compute landscape-level $R_{0,L}$ after having computed $R_{0,s,p}$ using equation S1 are the ratios of loss of infected rates b_{sp}/b_{tq}.

Assumptions regarding b_{sp}/b_{tq} ratios

Calculating landscape-level $R_{0,L}$ for an amphibian metacommunity required the ratios between the rates at which hosts left the infected class (i.e. b_{ij}/b_{sp} for $i, s = 1, \ldots, S$, $j, p = 1, \ldots, P$). We made the following two assumptions about the relative values of the rate of loss from the infected class b_{sp}. First, we assumed that recovery rates from Bd infection were inversely related to load, such that individuals with higher loads had a lower probability of clearing infection (Wilber *et al.* 2016; Ohmer *et al.* 2017). Second, we assumed loss of infection ν_{sp} occurred at a faster rate than background host mortality d_{sp} such that we could approximate b_{ij}/b_{sp} as a ratio of estimated mean Bd loads for species s in patch p μ_{sp}: $\frac{b_{ij}}{b_{sp}} = \frac{1/\mu_{ij}}{1/\mu_{sp}} = \frac{\mu_{sp}}{\mu_{ij}}$.

However, this assumption ignores the reality that the background death rate of amphibian larvae may be non-negligible (e.g. Vonesh & De la Cruz 2002). Consider $b_{sp} = d_{sp} + \nu_{sp}$ where d_{sp} is the background mortality rate and ν_{sp} is the recovery rate of larvae from species s in patch p. Our previous assumption was specifically that d_{sp} was small relative to the recovery rate ν_{sp}, which may not be true.

Now consider the ratio of two rates of removal from the infected class $\frac{b_1}{b_2} = \frac{d_1+\nu_1}{d_2+\nu_2}$. Note that we can re-write this equation as $\frac{b_1}{b_2} = \frac{\delta_1+1}{\frac{d_2}{d_1}\delta_1+\frac{\nu_2}{\nu_1}}$ where $\delta_1 = \frac{d_1}{\nu_1}$. This form of the ratio shows that, given some knowledge of the relative death rates d_2/d_1 and relative recovery rates ν_2/ν_1, the only information needed is the size of δ_1. For the results given in the main text, we assumed that $\delta_1 \to 0$ such that $\frac{b_1}{b_2} = \frac{\nu_1}{\nu_2}$. Here, we examined $\delta_1 = 1$ (i.e. death rate and recovery rate are on the same scale) and $\delta_1 = 10$ (i.e. death rate is larger than recovery rate) to see if our conclusions on the importance of maintenance species compared to source patches are robust to our assumption about background mortality rate.

To roughly approximate relative death rates of amphibian larvae, we used pace-of-life theory to hypothesize that amphibian larvae death rate for a species was proportional to reproductive output (Dammhahn *et al.* 2018). Specifically, we assumed that larvae of species that laid more eggs on average had a higher mortality rate. While approximate, this assumption allowed us to estimate relative death rates using published values on the number of eggs laid by amphibians per breeding season. The average number of eggs for each amphibian species was 5200 eggs for *A. boreas* (1 clutch), 2000 eggs for *R. draytonii* (1 clutch), 7000 eggs for *R. catesbeiana* (1 clutch), 200 eggs for *T. torosa* (over 4 clutches), 200 eggs for *T. granulosa* (unknown number of clutches), and 575 eggs for *P. regilla* (1 clutch, though can have up to 3 clutches) (values from University of California, Berkeley, USA 2019; Stebbins & McGinnis 2012).

We calculated the plausible connectivity parameter space for each metacommunty with the constraints that $\delta_1 = 0, 1,$ and 10, ratios of larvae death rates between host species were approximated by ratios of clutch sizes, ratios of loss of infection rates were approximated by 1 / estimated Bd loads, and $r_{sp} = \phi_s / b_{sp} < 1$. For each metacommunity, we drew 10,000 parameter sets where each parameter set was a $P \times H$ matrix of r_{sp} values satisfying the above constraints. We computed $R_{0,s,p}$ for each parameter set.

Once armed with 10,000 plausible parameter sets, we then, for each metacommunity, drew a plausible parameter set, computed landscape-level $R_{0,L}$ for each parameter set based on δ_1 and relative b_{sp} and ϕ_s values. We then separately removed either the most influential source patch or a particular species in the metacommunity and recomputed landscape-level $R_{0,L}$. For example, for a metacommunity with four species we computed six $R_{0,L}$ values for a given plausible parameter set: one baseline $R_{0,L}$, a removed $R_{0,L}$ for each of the four species, and a removed $R_{0,L}$ for the most influential source patch. The details on how we removed a species/patch are given below. We repeated this 100 times, randomly sampling from the plausible parameter space, and took the mean landscape-level $R_{0,L}$ values from these 100 simulations.

In summary, our results regarding the impact of species removals compared to source patch removals were not sensitive to our choice of background larvae mortality rates (Fig. S3, S4). In the main text, we present the results with $\delta_1 = 0$, which corresponds to a large loss of infection rate relative to background mortality rate.

Removing species and patches and re-computing $R_{0,L}$

To remove a species from a metacommunity, we can simply remove all of the rows and columns in $\mathbf{R}$ and $\mathbf{B}$ that are associated with the species of interest to obtain $\mathbf{R_{sdel}}$ and $\mathbf{B_{sdel}}$. $\mathbf{K_{sdel}}$ can then be calculated as above. For example, consider a metacommunity with $S = 3$ species and $P = 2$ patches. If we wanted to remove species 1, we would delete rows 1, 4 and columns 1, 4 in $\mathbf{R}$ and $\mathbf{B}$.

Removing a patch requires re-calculating $\mathbf{B}$ because the connectivity matrix $\mathbf{C}$ changes when a patch is deleted. The entry c_{ij} in $\mathbf{C}$ defines the probability of moving from patch $j \to i$ given a host moves somewhere, such that the sum of each column in $\mathbf{C}$ is one. Deleting patch p first requires setting all probabilities c_{pj} and c_{ip} in $\mathbf{C}$ to zero and re-normalizing the columns such that they sum to one. Note that the updated $\mathbf{C}'$ is still a $P \times P$ matrix. The matrix $\mathbf{B}'$ can then be calculated with the updated $\mathbf{C}'$. To complete the removal of patch p, we can remove rows and columns $(p-1)S + 1, \ldots, (p-1)S + S$ from $\mathbf{B}'$ and $\mathbf{R}$ to obtain $\mathbf{R_{pdel}}$ and $\mathbf{B_{pdel}}$. $\mathbf{K_{pdel}}$ can then be calculated as above.

References

Dammhahn, M., Dingemanse, N. J., Niemelä, P. T. & Réale, D. (2018). Pace-of-life syndromes: a framework for the adaptive integration of behaviour, physiology and life history. *Behav Ecol Sociobiol*, 72, 62.

Diekmann, O., Heesterbeek, J. A. P. & Metz, J. A. J. (1990). On the definition and the computation of the basic reproduction ratio R0 in models for infectious diseases in heterogeneous populations. *J Math Biol*, 28, 365–382.

DiRenzo, G. V., Campbell Grant, E. H., Longo, A. V., Che-Castaldo, C., Zamudio, K. R. & Lips, K. R. (2018). Imperfect pathogen detection from non-invasive skin swabs biases disease inference. *Methods Ecol Evol*, 9, 380–389.

DiRenzo, G. V., Langhammer, P. F., Zamudio, K. R. & Lips, K. R. (2014). Fungal infection intensity and zoospore output of *Atelopus zeteki*, a potential acute chytrid supershedder. *PLoS ONE*, 9, 1–6.

Fellers, G. M. & Kleeman, P. M. (2007). California red-legged frog (*Rana draytonii*) movement and habitat uses: implications for conservation. *J Herpetol*, 41, 276–286.

Fenton, A., Streicker, D. G., Petchey, O. L. & Pedersen, A. B. (2015). Are all hosts created equal? Partitioning host species contributions to parasite persistence in multihost communities. *Am Nat*, 186, 610–622.

Hanksi, I. (1999). *Metapopulation Ecology*. Oxford University Press, Oxford.

Joseph, M. B., Stutz, W. E. & Johnson, P. T. (2016). Multilevel models for the distribution of hosts and symbionts. *PLoS ONE*, 11, 1–15.

Marsh, D. M. & Trenham, P. C. (2001). Metapopulation dynamics and amphibian conservation. *Conserv Biol*, 15, 40–49.

Miller, D. A. W., Talley, B. L., Lips, K. R. & Campbell Grant, E. H. (2012). Estimating patterns and drivers of infection prevalence and intensity when detection is imperfect and sampling error occurs. *Methods Ecol Evol*, 3, 850–859.

Ohmer, M. E., Cramp, R. L., Russo, C. J., White, C. R. & Franklin, C. E. (2017). Skin sloughing in susceptible and resistant amphibians regulates infection with a fungal pathogen. *Sci Rep-UK*, 7, 3529.

Pimentel, R. A. (1960). Inter- and intrahabitat movements of the rough-skinned newt, *Taricha torosa granulosa* (Skilton). *Am Mdl Nat*, 63, 470–496.

277 Smith, M. A. & Green, D. M. (2005). Dispersal and the metapopulation paradigm in amphibian ecology
278 and conservation: are all amphibian populations metapopulations? *Ecography*, 28, 110–128.

279 Stebbins, R. C. & McGinnis, S. M. (2012). *Field Guide to Amphibians and Reptiles of California: Revised*
280 *Edition*. University of California Press, Berkeley, CA.

281 University of California, Berkeley, USA (2019). AmphibiaWeb. URL `https://amphibiaweb.org`.

282 Vonesh, J. R. & De la Cruz, O. (2002). Complex life cycles and density dependence: Assessing the contri-
283 bution of egg mortality to amphibian declines. *Oecologia*, 133, 325–333.

284 Wilber, M. Q., Langwig, K. E., Kilpatrick, A. M., McCallum, H. I. & Briggs, C. J. (2016). Integral Projection
285 Models for host-parasite systems with an application to amphibian chytrid fungus. *Methods Ecol Evol*, 7,
286 1182–1194.

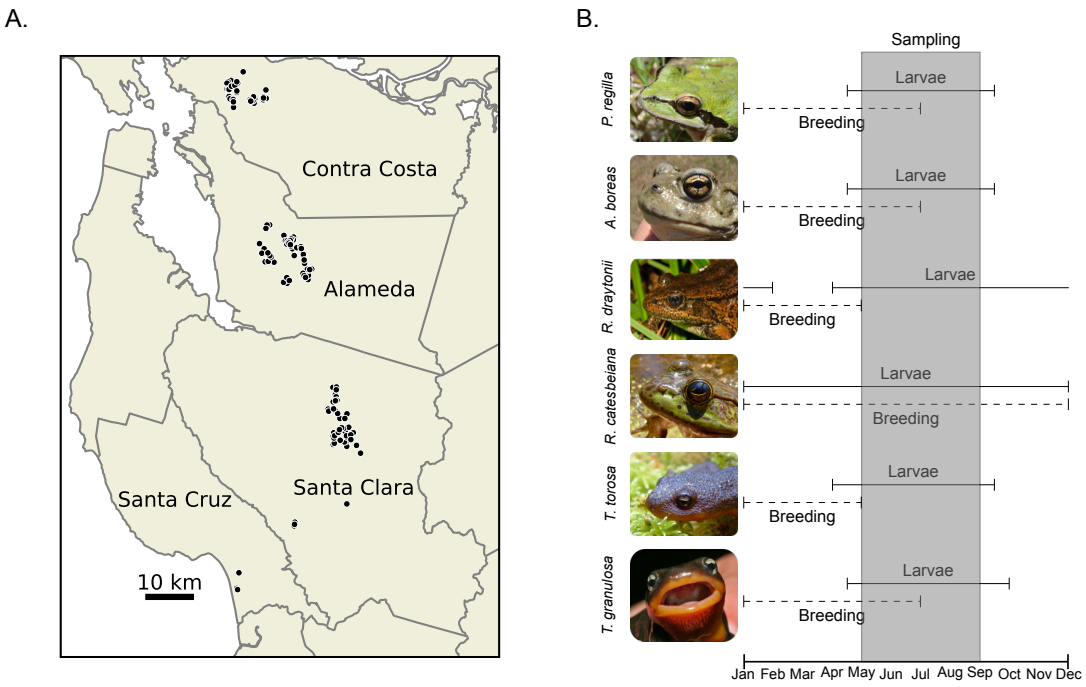

Figure S1: **A.** The unique ponds (patches) sampled in Contra Costa, Alameda, Santa Clara, and Santa Cruz counties in California, USA. There were also two ponds sampled in Monterey County (not shown). Black points are sampled ponds. White is water and brown is land **B.** The approximate timing of amphibian breeding and presence of larvae in ponds for the six amphibian species considered in this study. The gray region is the time of year when ponds were sampled for larval amphibian density and Bd prevalence.

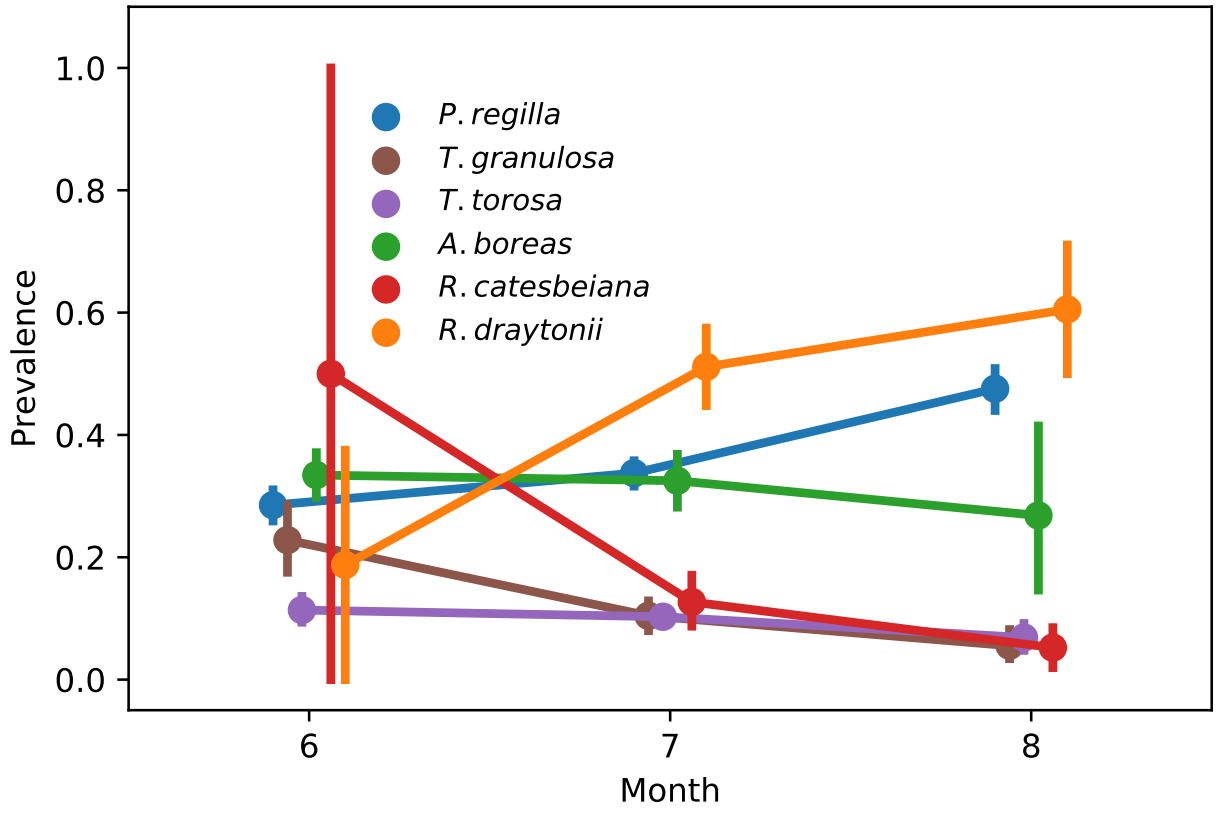

Figure S2: Plot of landscape-level prevalence in six amphibian species over the three months with the largest sampling effort from 2013-2018. Each point represents the mean prevalence of the amphibians sampled in that month. Sites were not sampled every month, so only a fraction of sites are represented in different points. Therefore, directly comparing across points is challenging. However, under an equilibrium assumption, we would expect relatively constant prevalences over the three months. In general, we do not see strong deviations from this expectation. While limited, this plot provides some evidence that there are not severe deviations from an endemic assumption at the landscape-level.

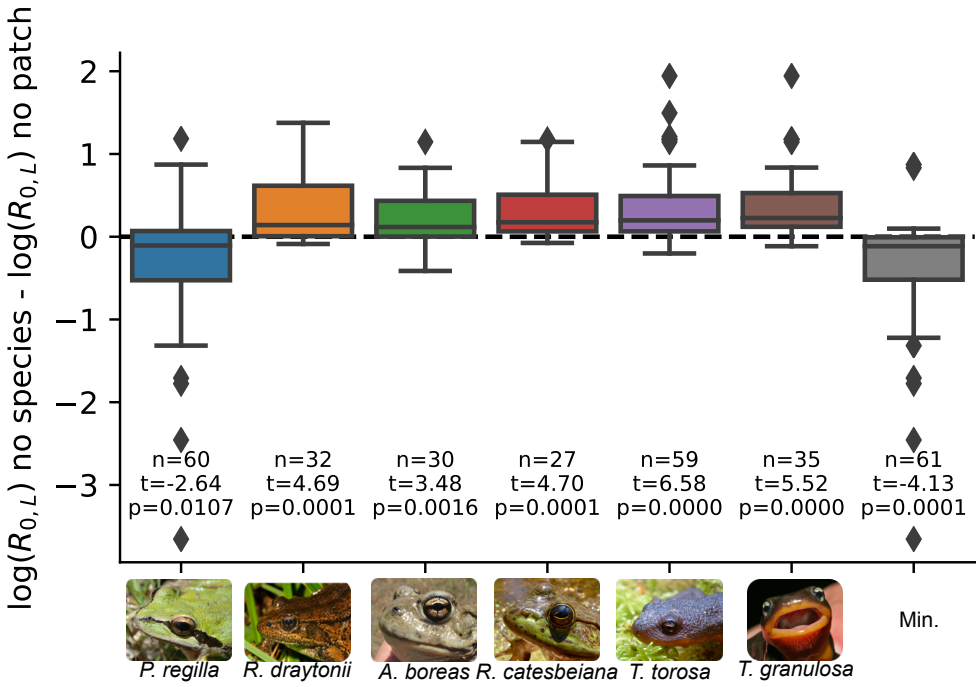

Figure S3: The effect of removing a species on landscape-level $R_{0,L}$ compared to removing the most influential source patch for 61 metacommunities with at least two patches and two species. Similar to Figure 5 in the main text, but the ratio between background mortality rate and loss of infection rate is set to one ($\delta_1 = 1$). Negative values indicate a larger reduction in landscape-level $R_{0,L}$ when a species is removed compared to when the most influential source patch is removed from the metacommunity. The sample sizes give the number of metacommunities out of 61 where a species was present. The t-statistics are from single sample t-tests testing the null hypothesis that the ratio $\log(\frac{R_{0,L}\text{no species}}{R_{0,L}\text{no patch}})$ is significantly different than zero. The p value is the significance value of the single sample t-test. The gray boxplot Min. shows the minimum ratio $\log(\frac{R_{0,L}\text{no species}}{R_{0,L}\text{no patch}})$ across all species within a given metacommunity. The dashed line indicates where removing a species and removing the most influential source patch have the same effect on landscape-level $R_{0,L}$.

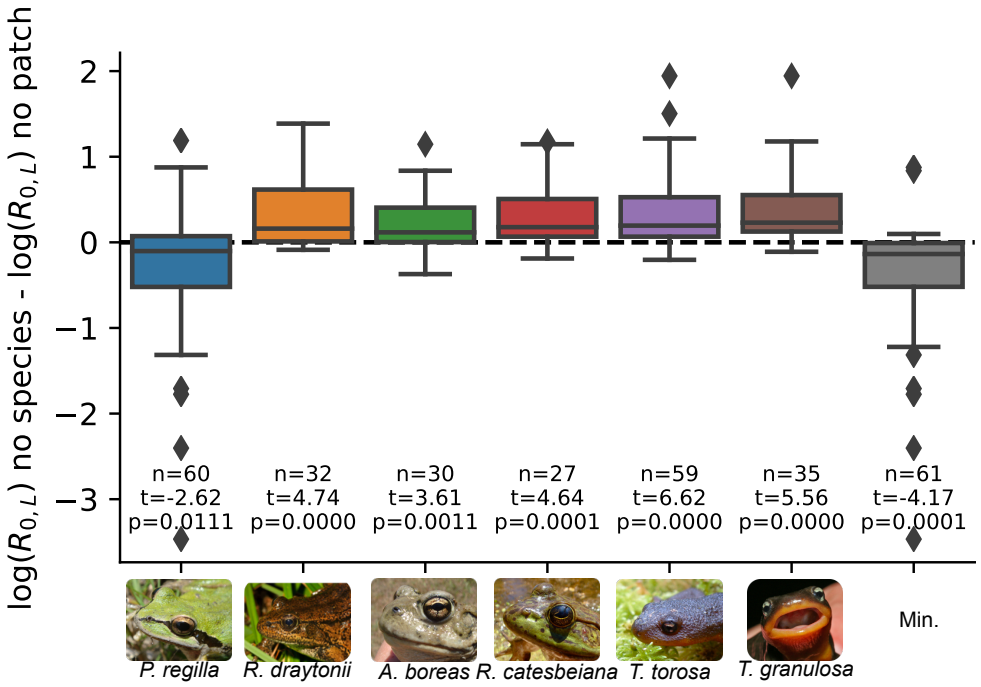

Figure S4: The effect of removing a species on landscape-level $R_{0,L}$ compared to removing the most influential source patch for 61 metacommunities with at least two patches and two species. Similar to Figure 5 in the main text, but the ratio between background mortality rate and loss of infection rate is set to 10 ($\delta_1 = 10$). Negative values indicate a larger reduction in landscape-level $R_{0,L}$ when a species is removed compared to when the most influential source patch is removed from the metacommunity. The sample sizes give the number of metacommunities out of 61 where a species was present. The t-statistics are from single sample t-tests testing the null hypothesis that the ratio $\log(\frac{R_{0,L}\text{no species}}{R_{0,L}\text{no patch}})$ is significantly different than zero. The p value is the significance value of the single sample t-test. The gray boxplot Min. shows the minimum ratio $\log(\frac{R_{0,L}\text{no species}}{R_{0,L}\text{no patch}})$ across all species within a given metacommunity. The dashed line indicates where removing a species and removing the most influential source patch have the same effect on landscape-level $R_{0,L}$.